Molecular Human Reproduction, Vol.15, No.12 pp. 829–842, 2009
Advanced Access publication on August 19, 2009 doi:10.1093/molehr/gap072

MHR Basic science of reproductive medicine

ORIGINAL RESEARCH

Genetic and gene expression analyses of the polycystic ovary syndrome candidate gene fibrillin-3 and other fibrillin family members in human ovaries

Mark J. Prodoehl[1], Nicholas Hatzirodos[1], Helen F. Irving-Rodgers[1], Zhen Z. Zhao[3], Jodie N. Painter[3], Theresa E. Hickey[1], Mark A. Gibson[2], William E. Rainey[4,5], Bruce R. Carr[5], Helen D. Mason[6], Robert J. Norman[1], Grant W. Montgomery[3], and Raymond J. Rodgers[1,7]

[1]Research Centre for Reproductive Health, Robinson Institute and School of Paediatrics and Reproductive Health, University of Adelaide, Adelaide, SA 5005, Australia [2]School of Medical Sciences, University of Adelaide, Adelaide, SA 5005, Australia [3]Molecular Epidemiology, Queensland Institute of Medical Research, Brisbane, QLD 4029, Australia [4]Department of Physiology, Medical College of Georgia, Augusta, GA 30912, USA [5]Division of Reproductive Endocrinology and Infertility, Department of Obstetrics and Gynecology, University of Texas Southwestern Medical Center at Dallas, Dallas, TX 75390-9032, USA [6]Division of Basic Medical Sciences, St. George's University of London, Cranmer Terrace, London SW17 0RE, UK

[7]Correspondence address. E-mail: ray.rodgers@adelaide.edu.au

ABSTRACT: Several studies have demonstrated an association between polycystic ovary syndrome (PCOS) and the dinucleotide repeat microsatellite marker D19S884, which is located in intron 55 of the fibrillin-3 (*FBN3*) gene. Fibrillins, including FBN1 and 2, interact with latent transforming growth factor (TGF)-β-binding proteins (LTBP) and thereby control the bioactivity of TGFβs. TGFβs stimulate fibroblast replication and collagen production. The PCOS ovarian phenotype includes increased stromal collagen and expansion of the ovarian cortex, features feasibly influenced by abnormal fibrillin expression. To examine a possible role of fibrillins in PCOS, particularly FBN3, we undertook tagging and functional single nucleotide polymorphism (SNP) analysis (32 SNPs including 10 that generate non-synonymous amino acid changes) using DNA from 173 PCOS patients and 194 controls. No SNP showed a significant association with PCOS and alleles of most SNPs showed almost identical population frequencies between PCOS and control subjects. No significant differences were observed for microsatellite D19S884. In human PCO stroma/cortex ($n = 4$) and non-PCO ovarian stroma ($n = 9$), follicles ($n = 3$) and corpora lutea ($n = 3$) and in human ovarian cancer cell lines (KGN, SKOV-3, OVCAR-3, OVCAR-5), *FBN1* mRNA levels were approximately 100 times greater than *FBN2* and 200–1000-fold greater than *FBN3*. Expression of *LTBP-1* mRNA was 3-fold greater than *LTBP-2*. We conclude that *FBN3* appears to have little involvement in PCOS but cannot rule out that other markers in the region of chromosome 19p13.2 are associated with PCOS or that *FBN3* expression occurs in other organs and that this may be influencing the PCOS phenotype.

Key words: fibrillin / latent-transforming growth factor β-binding protein / polycystic ovary syndrome / ovary

Introduction

Polycystic ovary syndrome (PCOS) is a common endocrine disorder that affects an estimated 5–7% of women of reproductive age in western societies and is characterized by hyperandrogenemia, chronic anovulation and polycystic ovaries (Knochenhauer *et al.*, 1998; Diamanti-Kandarakis *et al.*, 1999). Hirsuitism is common among women who suffer from the disorder, and they are at increased risk of anovulatory infertility, obesity (Conway *et al.*, 1989; Balen *et al.*, 1995), hyperlipidaemia and predisposing factors for heart disease (Wild *et al.*, 1985; Wild and Bartholomew, 1988; Slowinska-Srzednicka *et al.*, 1991; Wild *et al.*, 1992; Talbott *et al.*, 1995) and type II diabetes

(Knochenhauer *et al*., 1998; Diamanti-Kandarakis *et al*., 1999). While the aetiology of PCOS is unknown, familial studies have demonstrated heritability of the disorder, suggesting that there is a genetic component (reviewed in Amato and Simpson, 2004). Female first-degree relatives display strong association between the metabolic abnormalities of PCOS and hyperandrogenemia (Legro *et al*., 2002; Yildiz *et al*., 2003), and a recent study demonstrated that the brothers of women with PCOS also have a strong association with metabolic abnormalities (Urbanek *et al*., 2007). This suggests a common genetic association between the metabolic features of PCOS and hyperandrogenemia, whether that be a defect in the same gene or multiple genes in the same pathway.

The mode of inheritance of PCOS has proven difficult to determine suggesting that the disorder is a complex trait possibly involving multiple genes and/or environmental influences. Many genes in the steroid synthesis pathways (Carey *et al*., 1994; Gharani *et al*., 1997), the regulatory pathways of gonadotrophin action (Franks, 1995) and the insulin-signalling pathway have been investigated for association with the disorder. Many of these studies, however, have proven inconclusive or are not reproducible. In contrast, several studies using independent patient cohorts have demonstrated a significant association between PCOS and the dinucleotide repeat microsatellite marker D19S884, which is located 1cM upstream of the insulin receptor (*INSR*) gene in chromosome region19p13.2 (Tucci *et al*., 2001; Villuendas *et al*., 2003; Urbanek *et al*., 2005; Urbanek *et al*., 2007). The distance of this marker from *INSR* casts doubt upon the likelihood of there being a causal genetic variant within *INSR* and it is more probable that variant(s) in a distal enhancer of *INSR* or an unrelated gene are the reason for the association between D19S884 and PCOS. D19S884 is located within intron 55 of the fibrillin-3 gene (*FBN3*).

Fibrillins and latent TGF-β-binding proteins (LTBPs) form a family of proteins that are characterized by a modular domain structure comprising epidermal growth factor-like (EGF) domains, calcium-binding EGF domains and unique cysteine-rich TB domains. Three fibrillin genes, *FBN1, 2* and *3* (Sakai *et al*., 1986; Lee *et al*., 1991; Corson *et al*., 2004), and four LTBP genes, *LTBP 1, 2, 3* and *4* (Kanzaki *et al*., 1990; Moren *et al*., 1994; Yin *et al*., 1995; Giltay *et al*., 1997), have been identified in mammals, although in rodents *FBN3* has been disrupted due to chromosomal rearrangements (Corson *et al*., 2004). *FBN3* is most highly expressed in human fetal tissues and the human adult brain, eye, lung, adrenal glands, stomach and ovaries (Wheeler *et al*., 2003; Corson *et al*., 2004). Studies of *FBN1* and *2* have shown that they function as structural components of elastin fibres or mircrofibrils and as regulators of TGF-β family members. Regulation of TGF-β activity by the fibrillins is a result of their ability to bind to LTBPs causing sequestration of latent TGF-βs into the extracellular matrix where they are stored and/or activated (Ramirez and Pereira, 1999; Kielty *et al*., 2002; Neptune *et al*., 2003). However, there are subtle differences between them. For instance, LTBP-2 itself does not bind latent TGF-βs (Gibson *et al*., 1995), but can competitively replace LTBP-1 bound to FBN1 (Hirani *et al*., 2007). LTBPs are also required for the correct secretion and folding of TGF-βs (Miyazono *et al*., 1991). To date, interactions between FBN3 and LTBPs have not been investigated. Clinical consequences of the disruption of the interaction between the fibrillins and TGF-βs have been reported previously in the pathogenesis of Marfan's syndrome, a connective tissue disorder affecting the limbs, the heart, the lungs and the eyes. Mutations in *FBN1* or the TGF-β type 2 receptor cause Marfan's syndrome (Boileau *et al*., 2005). The ability of mutations in *FBN1* to phenocopy those in TGF-βR type 2 suggests that the structural role of FBN1 in the formation of elastic fibres and microfibrils is less critical to the pathology of the disease than its role in regulating the bioavailability of TGF-β family members.

The involvement of the TGF-β superfamily in the development of PCOS has been implied from functional data (Glister *et al*., 2005, 2006) and the association of several members, including anti-Mullerian hormone (AMH), activin, inhibin and their associated receptors, as well as follistatin, and the SMADS, has been examined (Urbanek *et al*., 1999; Urbanek *et al*., 2000; Kevenaar *et al*., 2008). Strong association of these genes with PCOS has not been demonstrated, however, it has been suggested that both follistatin, which like fibrillins and LTBPs, contain a TB domain (Thompson *et al*., 2005), and AMH may contribute to the severity of the PCOS phenotype by influencing androgen levels and/or follicle development (Urbanek *et al*., 2000; Jones *et al*., 2007; Kevenaar *et al*., 2008). Women with PCOS not only display aberrant follicle maturation, but also develop a thickening of the tunica albuginea and stromal tissues of their ovaries that is associated with an increase of collagen deposition in these regions (Hughesdon, 1982). TGF-β superfamily members have been implicated in the regulation of collagen synthesis by fibroblasts in fibroses; TGF-β promotes collagen expression and fibrosis while bone morphogenic protein (BMP)7 suppresses these effects (Govinden and Bhoola, 2003; Wang *et al*., 2003; Zeisberg *et al*., 2003; Verrecchia and Mauviel, 2004; Christner and Ayitey, 2006). Hence we have considered the possibility that the fibrillin/LTBP protein family members may be involved in both the gross ovarian morphological and follicular developmental defects associated with PCOS through a disruption in fibrillin-LTBP interactions resulting in perturbations in TGF-β signalling pathways. For these reasons, we chose to undertake a case–control PCOS association test of 32 single nucleotide polymorphisms (SNPs) within *FBN3*. We included non-synonymous SNPs located in the coding region of the gene with the aim of identifying PCOS-associated *FBN3* variants that may lead to disrupted protein function. We also examined the RNA expression profiles of fibrillin/LTBP family members in human ovarian tissues and cell lines.

Materials and Methods

Subjects for DNA genotyping

Ethics approval for this study was obtained from the University of Adelaide Human Research Ethics Committee. Case subjects were recruited from infertility and antenatal clinics at The Queen Elizabeth Hospital in Adelaide, South Australia, after approval by the ethics committee of North Western Adelaide Health Services. Details of a number of these subjects have been reported previously (Milner *et al*. 1999). The study group represented women of various European cultural backgrounds who generally can be classified as Caucasian. Case subjects consisted of women with PCOS defined as hyperandrogenism and chronic anovulation as per the 1990 NIH consensus criteria (Zawadski and Dunaif, 1992). Polycystic ovaries were identified on ultrasound and defined as the presence of at least eight peripheral cysts less than 10 mm in diameter, with increased ovarian stroma occurring bilaterally (Adams *et al*., 1986). A total of 367 women between the ages of 18 and 42 were recruited and of these, 173 (47%) women fulfilled the criteria for PCOS. A further 86 patients

from the same clinics but who had none of the characteristics of PCOS, and largely male-factor related reasons for infertility, served as controls. An additional 108 patients whose PCO status was unknown were recruited from the female blood donor population (Milner *et al*., 1999). All samples were de-identified for further analysis.

DNA extraction

Peripheral blood lymphocytes were purified from whole blood using Lymphoprep (Nycomed Pharma, Oslo, Norway) and kept frozen in saline at −20°C until DNA extraction. DNA was extracted from this tissue using a DNeasy Kit (QIAGEN, Chatsworth, CA) as per the manufacturer's protocol, quantified by spectrophotometry and stored at −20°C.

Analyses of SNPs

We typed a single multiplex of 32 tagging and functional SNPs spanning an 82 kb region of *FBN3*. Tagging SNPs (a set of SNPs that through high linkage disequilibrium (LD) capture the variation in other common SNPs in the region) were chosen using genotyping data from the International HapMap Project (http://www.hapmap.org/) from a population of Caucasian and European background (CEU), having minor allelic frequencies of >0.05 and r^2 values of >0.8. Additional functional SNPs that produce a change in protein sequence were chosen to complete the multiplex using genotyping data from the SNP database at the National Library of Medicine (http://www.ncbi.nlm.nih.gov/snp), such that they would not interfere with the multiplexing of the tagging SNPs. All SNP sequences were downloaded from the Chip Bioinformatics database (http://snpper.chip.org/) and the sequences were cross checked with the National Center for Biotechnology Information (NCBI, http://www.ncbi.nlm.nih.gov/) and Sequenom RealSNP databases (https://www.realsnp.com/) before assay design. Assays were designed for the 32 SNPs using the Sequenom MassARRAY Assay Design software (version 3.1). SNPs were typed using iPLEX ™ Gold chemistry and analysed using a Sequenom MassARRAY Compact Mass Spectrometer (Sequenom Inc, San Diego, CA , USA). The 2.5 μL PCR reactions were performed in standard 384-well plates using 12.5 ng genomic DNA, 0.8 unit of *Taq* polymerase (HotStarTaq, Qiagen, Valencia, CA), 500 μmol of each dNTP, 1.625 mM of $MgCl_2$ and 100 nmol of each PCR primer (Bioneer, Daejeon, Korea). PCR thermal cycling in an ABI-9700 instrument was 15 min at 94°C, followed by 45 cycles of 20 s at 94°C, 30 s at 56°C and 60 s at 72°C. To the completed PCR reaction, 0.15 U shrimp alkaline phosphatase was added and incubated for 40 min at 37°C followed by inactivation for 5 min at 85°C. A mixture of extension primers was tested to adjust the concentrations of extension primers to equilibrate signal-to-noise ratios in the matrix-assisted laser desorption/ionization − time of flight (MALDI-TOF) mass spectrometry prior to use for extension reactions. The post-PCR reactions were performed in a final 5 μl of extension reaction containing 1× termination mix, 1 U DNA polymerase and 570– 1240 nM extension primers. A two-step 200 short cycle programme was used for the iPLEX Gold reaction as described in a previously study (Zhao *et al*., 2006). The iPLEX reaction products were desalted by diluting samples with 15 μl of water and adding 5 μl of resin (Sequenom Inc, San Diego, CA, USA). The products were spotted on a SpectroChip (Sequenom Inc), and data were processed and analysed by MassARRAY TYPER 3.4 software (Sequenom Inc).

Microsatellite genotyping

To detect microsatellite D19S884 alleles we designed our own primers (Table I) rather than using those suggested for amplimer AFMa299zc5 listed in Genbank as we found these to be unreliable. Primers were designed using Primer Express software (Applied Biosystems, Foster City, CA, USA), from the published genomic sequence of human *FBN3* (Table I). The amplification reactions were performed using 50 ng genomic DNA, 1 U of *Taq* polymerase (AmpliTaq Gold, PE Applied Biosystems) in 1.56 mM $MgCl_2$, 0.1 mM of each dNTP and 10 nmol of each primer. The cycling conditions were 95°C initially for 7 min followed by 40 cycles of 95°C, 55°C and 72°C of 30 s each, then a final extension of 30 min at 72°C. The fluorescent PCR products were assayed by capillary electrophoresis and visually analysed using the ABI 3730 DNA Analyser (Applied Biosystems) with GeneScan Analysis software. Allele lengths were confirmed by DNA sequencing of homozygous alleles.

Statistical analyses

LD analyses and pairwise LD plots of D' were generated using the Haploview 3.32 software (http://www.broad.mit.edu/haploview/haploview) (Barrett *et al*., 2005). The statistical power to detect an association in our case–control cohort was calculated by post-hoc tests implemented in the G.Power software (Buchner *et al*., 1997) for an alpha (*P*-value) of 0.05 over effect sizes ranging from 0.1 (small) to 0.5 (medium). The sample has 60% power to detect an effect size of 0.2 and greater than 88% power for effect sizes of 0.3 or more. Case–control association tests for SNP markers were performed using unphased 3.0.10 (Dudbridge, 2008). Odds ratios (ORs) with corresponding 95% confidence intervals (95% CI) were calculated using Woolf's formula with Haldane's correction. *P*-values were corrected for multiple comparisons using Bonferroni's correction. Case–control association tests for the microsatellite marker D19S884 were performed using Clump 2.3 (www.mds.qmw.ac.uk/statgen/dcurtis/software.html) and Fisher's exact test. *P*-values for Fisher's exact tests were calculated using GraphPad Prism 5.00 for Windows (GraphPad Software, San Diego California USA,

Table I Primers used for qRT–PCR and microsatellite genotyping

Gene or locus	Genebank accession number	Location of amplicon	Forward primer (5′–3′)	Reverse primer (5′–3′)
18S	AF176811	56–146	AGAAACGGCTACCACATCCAA	CCTGTATTGTTATTTTTCGTCACTACC
FBN1	BC146854	1822-1882	AGCACACTCACGCGGACA	AGATCCGGCCATTCTGTAAACA
FBN2	NM_001999	7545-7646	TCCAGTCAAGTTCTTCAGGCAC	TGCGACTACTGGATGCCATTT
FBN3	NM_032447	1716-1787	TGGCGGCCACTACTGCAT	TTGGTACAGTGGCCGTTCAC
LTBP-1	BC130289	3195-3322	CCCCAATGTCACGAAACAAGA	AACCTTTCCCTTTGGGACACA
LTBP-2	NM_000428	3276-3382	CAGGAAAGGACACTGCCAAGA	CCTCACAGGCCAGACAAGTGTA
D19S884	NC_000019	62 185–62 353	GGAGTTGCTCAGGGTC	TCCCTCAACCCCCCGAGTTC

www.graphpad.com) and were Bonferroni corrected for multiple comparisons.

Tissues for gene expression analyses

Collection of tissues for gene expression analyses was approved by the Institution Review Boards of the University of Texas Southwestern Medical Center, Dallas, USA, St Georges University of London, England and The University of Adelaide, Australia. Informed written consent was obtained prior to collection of tissues. Tissues were obtained from premenopausal women undergoing procedures for benign gynaecologic conditions. PCOS ovarian phenotype was diagnosed based on the presence of three or more of the following criteria: enlarged ovarian volume (>9 ml), 10 or more follicles of 2–8 mm in diameter, increased density and volume of stroma or a thickened tunica (Mason *et al.*, 1994). Specimens were obtained from ovarian stroma/cortex ($n = 9$ non-PCO and 4 PCO ovarian phenotype), ovarian follicles ($n = 3$, >8 mm diameter) and corpora lutea ($n = 3$). The human ovarian cancer cell lines OVCAR-3, OVCAR-5 and SKOV-3 (ascites derived) originating from ovarian adenocarcinomas were obtained from the ATCC (Manassas, VA, USA) and the granulosa tumour cell line KGN (Nishi *et al.*, 2001) was obtained with consent from its originators Professors Hajime Nawata and Toshihiko Yanase of Kyushu University and Professor Yoshihiro Nishi of Kurume University. Tissues and cells were either stored in RNAlater (Ambion, Inc., Austin, TX) at −20°C, or snap frozen in liquid nitrogen and stored at −80°C prior to RNA or protein isolation.

Gene expression analyses

Total RNA was isolated from ~100 mg wet weight of stored stromal tissue using 1 ml of Trizol (Invitrogen Australia Pty. Ltd., Mt Waverley, VIC, Australia). Briefly, tissue was homogenized for approximately 30 s on ice using a polytron homogenizer before extraction was carried out as per manufacturer's instructions. Ten micrograms of total RNA was treated with 2 U of DNase I (Ambion Inc, Austin, TX, USA) and first-strand complementary DNA (cDNA) was synthesized from the DNase-treated RNA (2.5 μg) using 200 U Superscript III reverse transcriptase (Invitrogen Australia Pty. Ltd.) and 500 ng random hexamers (Geneworks, Thebarton, SA, Australia). Primers were designed against published mRNA sequences using Primer Express software (Applied Biosystems). Primer sequences for human *FBN1, 2* and *3* and, *LTBP-1* and *-2* mRNA are shown in Table I. Real-time PCR amplification was performed using an ABI PRISM 7000 sequence detection system (Applied Biosystems) by adding 2.5 μl of appropriately diluted cDNA, 10 μl 2× SYBR green master mix (Applied Biosystems), 7.1 μl water and 0.2 μl of 12.5 μM forward and reverse primers per well. Samples were amplified in duplicate for one cycle at 50°C for 2 min and 95°C for 10 min, followed by 40 cycles of 95°C for 15 s and 60°C for 1 min.

To generate a standard curve for each PCR assay, DNA standards for each target sequence were prepared by sub-cloning the PCR products of the corresponding target sequence into pCR2.1-TOPO vector (Invitrogen). The plasmid DNA was isolated and quantified using a Nanodrop spectrophotometer (Nanodrop technologies, Wilmington, DE, USA). DNA sequences were verified by automated sequencing (3730 DNA analyser, Applied Biosystems). Concentrations were calculated from absorbance at 260 nm. Plasmid DNA was serially diluted over three logs to establish a standard curve in a range, determined for each sample, which bounded the C_T values obtained for samples (between 1 ng/μl and 10 ag/μl). Concentration of each target was generated from the C_T and standard curve and was normalized to the concentration of 18S ribosomal RNA in each sample (calculated by the C_T and standard curve for 18S). Gene expression of target sequences was subsequently expressed as fmoles target sequence mRNA/nmole 18S ribosomal RNA. For each gene the expression levels were normally distributed and comparisons between each ovarian compartment and between PCO and non-PCO tissues were compared by ANOVA, with no *post hoc* tests necessary as no significant differences were found.

Results

SNP and microsatellite analyses

Marker selection

We successfully genotyped 173 PCOS patients and 194 healthy control subjects for 32 SNPs (Table II) within 82 kb of the *FBN3* gene region (gene map in Fig. 1). We included SNPs ($n = 10$) that result in non-synonymous amino acid changes in the FBN3 protein (Table II), with the intention of identifying PCOS-associated *FBN3* mutations that might lead to defects in the functioning of the FBN3 protein either pre- or post-translationally. One SNP (rs17202741) showed no heterogeneity in the population and another (rs12972954) showed significant departures from Hardy–Weinberg equilibrium (possibly indicating a problem with the primers used for genotyping). Both were subsequently excluded from further analyses.

SNP association analyses

The results of the Sequenom genotyping analysis are displayed in Table III. Relative frequencies for each allele of the 30 SNPs analysed from PCOS and control subjects are summarized. Most alleles showed almost identical population frequencies between PCOS and control subjects. SNP association analyses performed with unphased software (Dudbridge, 2008) found only one SNP (rs3813774) that achieved a significant ($P = 0.04$ uncorrected) association with PCOS (Fig. 1). In addition, case–control association analysis with Haploview software (Barrett *et al.*, 2005) found one SNP (rs3813774) that achieved a significant ($P = 0.04$ uncorrected) association with PCOS (Table III). Upon correction for multiple comparisons, however, the *P*-value for this SNP no longer reached significance.

Haplotype association and linkage analyses

In order to increase the potential to identify a PCOS-associated SNP in the *FBN3* genomic region we also performed LD haplotype association analyses using Haploview software (Barrett *et al.*, 2005). Haplotype association analysis can increase power to detect a signal from other unknown SNPs (not in current databases) by performing the association test on haplotype groups rather than individual SNPs. Four haplotype blocks with 18 haplotypes were identified by Haploview using the method described by Gabriel *et al.* (2002) (Fig. 2a). Haplotype association frequencies, haplotype population frequencies and *D′* scores of these haplotype blocks are shown in Fig. 2. Haplotype analysis failed to identify haplotypes that show significant association with PCOS. Given that the marker that led us to examine SNPs in *FBN3* (the microsatellite D19S884) is located in a region of low LD (Fig. 2 and Urbanek *et al.*, 2007), this result is perhaps not surprising as haplotype blocks do not by definition exist in regions of low LD.

Microsatellite D19S884 association analysis

As we were unable to demonstrate association between the SNPs that we typed in the *FBN3* region and PCOS, we decided to genotype our patient–control cohort for the previously associated microsatellite

Table II Information on the SNPs examined, including chromosomal and gene location, sequence variation and the frequencies of their minor alleles for both control and PCOS patients, and the *P*-value for deviation of the genotype frequencies from the Hardy–Weinberg equilibrium

Public id[a]	Chromsomal location[b]	Gene location	Variation#	Minor allele#	Hardy–Weinberg *P*-value[c]	Allele frequency[d]	
						Control	Case
rs2287937	8036420	3′ UTR	G/C	G	1.00	0.19	0.23
†rs12972954	8037849	Intronic	C/T	T	–	–	–
rs10424096	8041170	Intronic	A/G	G	0.36	0.07	0.07
rs17261710	8042398	Intronic	C/T	C	0.67	0.17	0.18
rs2303169	8052114	Intronic	G/A	A	0.06	0.44	0.47
rs17160147	8054042	Intronic	G/C	C	0.17	0.70	0.71
††rs17202741	8062366	Coding	A/C AUG(M), CUG(L)	C	–	–	–
rs12151028	8064924	Intronic	G/C	C	0.06	0.86	0.88
rs7245429	8065362	Coding	C/A CCT(P), CAT(H)	A	0.57	0.40	0.42
rs7245552	8065409	Silent	C/A CCC(P), CCA(P)	C	0.89	0.64	0.64
rs12608849	8066334	Coding	T/C TTC(F), ATC(I)	T	0.76	0.25	0.28
rs12150963	8066897	Coding	G/C AAC(N), AAG(K)	G	0.07	0.86	0.87
rs3829817	8067450	Coding	G/A CGG(R), CAG(Q)	A	0.71	0.75	0.77
rs3865464	8074340	Intronic	C/T	T	0.68	0.88	0.90
rs33967815	8074545	Coding	G/A GGC(G), AGC(S)	A	0.22	0.31	0.32
rs10445638	8079428	Intronic	G/A	A	0.84	0.09	0.09
rs3813779	8080650	Intronic	C/T	T	0.23	0.53	0.56
rs8111335	8082361	Intronic	T/C	T	0.74	0.14	0.17
rs12975322	8082640	Coding	G/A GTC(V), ATC(I)	A	0.36	0.75	0.78
rs4804063	8082945	Coding	G/A AGT(S), GGT(G)	G	0.41	0.81	0.83
rs2086149	8083620	Intronic	A/G	A	0.27	0.30	0.30
rs35579498	8089871	Coding	C/T CGG(R), TGG(W)	T	0.86	0.04	0.04
rs4527136	8092519	Intronic	C/T	T	1.00	0.44	0.47
rs35840170	8094812	Coding	G/A GTC(V), ATC(I)	A	1.00	0.97	0.97
rs3813774	8102499	Silent	C/T TGC(C), TGT(C)	T	0.35	0.05	0.08
rs12974280	8102508	Silent	C/G TCC(S), TCG(S)	G	0.57	0.62	0.64
rs8112525	8107051	Intronic	G/A	A	0.04	0.09	0.10
rs2061776	8108373	Intronic	A/G	A	0.13	0.84	0.85
rs7246376	8109328	Coding	C/T CCC(P), CTC(L)	T	0.42	0.80	0.80
rs12162237	8113070	Intronic	T/C	T	0.77	0.44	0.48
rs7252584	8113241	Intronic	G/C	C	0.64	0.15	0.20
rs7256533	8113721	Intronic	T/C	T	1.00	0.54	0.56

[a]Reference SNP cluster identification number.
[b]Position of nucleotide on chromosome 19 in Build 35 of the human genome from UCSC (www.genome.ucsc.edu).
[c]*P*-value for deviation of genotype frequencies from Hardy–Weinberg equilibrium.
[d]Minor allelic frequency calculated using Haploview software.
†SNP displaying significant departure from Hardy–Weinberg equilibrium.
††Potential SNP found not to be allelic. # The bases listed are those used in our design of primers and may represent the complimentary bases as listed in the Public Id.

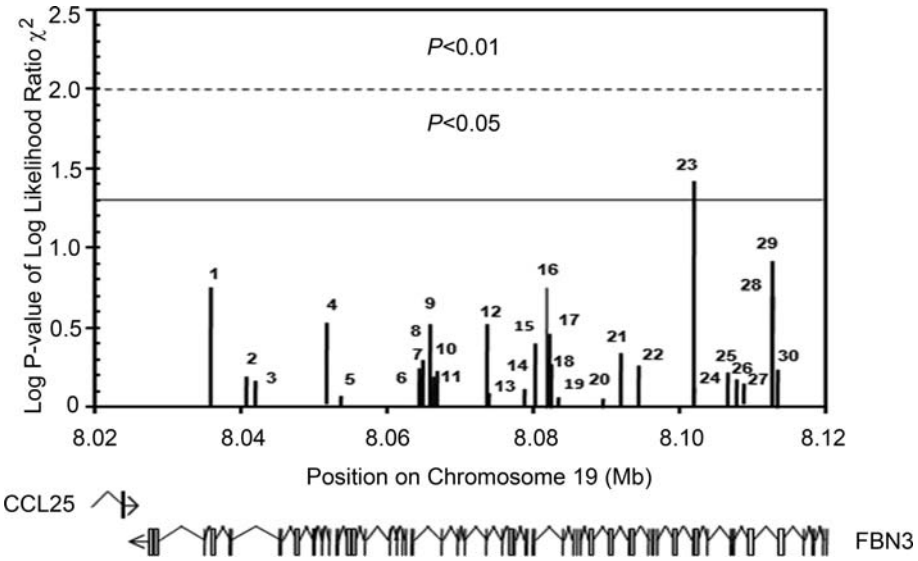

Figure 1 Unphased association analysis for 30 SNPs all of which can be mapped within an 82 kb region spanning *FBN3*. Chromosomal position is plotted versus −log *P*-value for chi-square tests of association of each marker with PCOS. The dotted lines represent the cut-off mark for *P*-values reaching significance before Bonferroni's correction for multiple testing ($P \leq 0.05$ and $P \leq 0.01$). The position of introns and exons of the two genes (*CCL25* and *FBN3*) relative to the SNPs analysed are displayed below the graph. Markers are 1 rs2287936, 2 rs10424096, 3 rs17261710, 4 rs2303169, 5 rs17160147, 6 rs12151028, 7 rs7245429, 8 rs7245552, 9 rs12608849, 10 rs12150963, 11 rs3829817, 12 rs3865464, 13 rs33967815, 14 rs10445638, 15 rs3813779, 16 rs8111335, 17 rs12975322, 18 rs4804063, 19 rs2086149, 20 rs35579498, 21 rs4527136, 22 rs35840170, 23 rs3813774, 24 rs12974280, 25 rs8112525, 26 rs2061776, 27 rs7246376, 28 rs12162237, 29 rs7252584 and 30 rs7256533.

marker D19S884. Microsatellite D19S884 allele frequencies for the study group are shown in Table IV. The numbers of CA repeats ranged from 14 to 24 in our cohort, and repeats of 22, 17, 18 and 20 were the most common at 26–27, 17, 12–13 and 11%, respectively. The frequencies of each allele reported here are similar to those published previously (Table IV).

Microsatellite allele association analyses were performed using Fisher's exact test and the Clump program. Fisher's exact test did not identify any alleles of D19S884 that were significantly associated with PCOS. Allele 10 (19 CA repeats) was the only allele that was significant ($P = 0.04$ uncorrected), however, upon correction for multiple testing this *P*-value no longer approached significance ($P = 0.52$) (Table IV). Clump analysis of D19S884 failed to identify association between any of the 11 alleles detected and PCOS (data not shown).

FBN and LTBP expression in human ovaries

We examined the expression of *FBN1, 2 and 3* (Fig. 3), and *LTBP-1* and -2 mRNA (Fig. 4) in normal human ovarian tissues including stroma/cortex ($n = 9$ non-PCO and 4 PCO ovarian phenotype), follicles ($n = 3$) and corpora lutea ($n = 3$) and ovarian cell lines. Expression levels for each gene were not significantly different between stroma, follicles and corpora lutea. *FBN1* mRNA levels were 50–100 times greater than *FBN2* and 200–1000-fold higher than *FBN3* (Fig. 3). The granulosa tumour cell line KGN displayed similar levels of *FBN1* and 2 but lower levels of *FBN3* expression when compared with normal ovarian tissue samples (Fig. 3). OVCAR-3, OVCAR-5 and SKOV-3 had lower levels of *FBN1* than normal ovarian tissues and KGN cells (Fig. 3). OVCAR-3 cells had very high levels of expression of both *FBN2* and *3* expression compared with the other cell lines and the ovarian tissues (Fig. 3).

LTBP-1 expression levels were >3-fold greater than *LTBP-2* in normal ovarian tissues (Fig. 4). OVCAR-3, OVCAR-5 and SKOV-3 had lower levels of *LTBP-2* than normal ovarian tissues, but *LTBP-1* expression was variable across the cell lines; with OVCAR-3 having the highest levels of expression (Fig. 4). Correlation analyses were conducted and *FBN1* expression significantly correlated with *FBN2* ($P < 0.001$) and LT*BP-1* ($P < 0.01$) and *FBN2* with *LTBP-1* ($P < 0.001$) across all tissues (Fig. 5).

Discussion

We have conducted a case–control study of PCOS examining the genotypes of 30 SNPs, including 10 functional SNPs, in an 82 kb region of chromosome 19 flanking *FBN3*. In our cohort, we also genotyped the microsatellite marker D19S884, previously reported to be associated with PCOS by familial linkage analyses and located within intron 55 of *FBN3*. In addition, we examined the expression of the three *FBN*s and two of the *LTBP*s (*LTBP-1* and -2) in ovarian tissues. We conclude that if *FBN3* is involved in the aetiology of PCOS then its role is not readily apparent from these studies.

Tagging SNPs were chosen to span an 82 kb region of the *FBN3* gene, which flanks the previously associated microsatellite marker D19S884, such that ~100% of SNP alleles with minor allele frequencies >5% in this region were captured with an r^2 value of >0.8. Thus, we would have expected to have been able to identify any common SNP within this region of 19p13.2 that showed significant association

Table III Association analysis of SNPs within the *FBN3* gene with PCOS showing chromosomal position, chi-square values, *P*-values, odds ratios, confidence limits and allelic frequencies for each SNP

Marker id[a]	Chromosomal postion[b]	χ^2 (Haploview)[c]	*P*-value (Haploview)[d]	−log *P*-value	Odds ratio[e]	95% low[f]	95% high[g]	*P*-value corrected (Haploview)[h]	Minor allele				Major allele			
									Case frequency	Control frequency	Case number[i]	Control number[j]	Case frequency	Control frequency	Case number[i]	Control number[j]
rs2297936	8036420	1.81 (1.92)	0.18 (0.17)	0.74	1.28	0.89	1.83	1 (1)	0.23	0.19	80	74	0.77	0.81	266	314
rs10424096	8041170	0.21 (0.11)	0.64 (0.74)	0.19	1.15	0.64	2.04	1 (1)	0.07	0.07	25	24	0.93	0.93	311	342
rs17261710	8042398	0.17 (0.20)	0.68 (0.66)	0.17	0.92	0.63	1.35	1 (1)	0.18	0.16	61	64	0.82	0.84	285	324
rs2303169	8052114	1.08 (1.08)	0.30 (0.30)	0.52	0.86	0.63	1.17	1 (1)	0.47	0.44	163	169	0.53	0.56	181	219
rs17160147	8054042	0.03 (0.03)	0.85 (0.85)	0.07	1.03	0.74	1.43	1 (1)	0.30	0.30	101	117	0.70	0.70	241	271
rs12151028	8064924	0.32 (0.32)	0.57 (0.57)	0.24	1.13	0.72	1.77	1 (1)	0.13	0.14	43	54	0.88	0.86	301	334
rs7245429	8065362	0.41 (0.41)	0.52 (0.52)	0.28	0.91	0.67	1.22	1 (1)	0.42	0.39	142	153	0.58	0.61	198	235
rs7245552	8065409	0.002 (0.002)	0.96 (0.96)	0.02	0.99	0.73	1.35	1 (1)	0.36	0.36	121	138	0.64	0.64	219	248
rs12608849	8066334	1.05 (1.05)	0.31 (0.31)	0.51	1.19	0.86	1.64	1 (1)	0.28	0.25	97	96	0.72	0.75	245	288
rs12150963	8066897	0.21 (0.21)	0.65 (0.65)	0.19	0.90	0.58	1.42	1 (1)	0.13	0.14	43	53	0.87	0.86	299	333
rs3829817	8067450	0.26 (0.22)	0.61 (0.64)	0.21	1.09	0.78	1.54	1 (1)	0.23	0.25	80	96	0.77	0.75	266	292
rs3865464	8074340	1.08 (1.08)	0.30 (0.30)	0.52	0.78	0.50	1.23	1 (1)	0.10	0.12	34	48	0.90	0.88	308	340
rs33967815	8074545	0.03 (0.06)	0.85 (0.81)	0.07	1.03	0.76	1.40	1 (1)	0.32	0.31	111	122	0.68	0.69	235	266
rs10445638	8079428	0.07 (0.07)	0.79 (0.79)	0.10	0.93	0.55	1.57	1 (1)	0.09	0.09	31	33	0.91	0.91	309	353
rs3813779	8080650	0.68 (0.57)	0.41 (45)	0.39	0.88	0.67	1.18	1 (1)	0.44	0.47	150	181	0.56	0.53	194	207
rs8111335	8082361	1.80 (1.81)	0.18 (0.18)	0.74	1.32	0.86	2.02	1 (1)	0.17	0.14	59	53	0.83	0.86	283	335
rs12975322	8082640	0.88 (0.88)	0.35 (0.35)	0.46	1.18	0.83	1.67	1 (1)	0.22	0.25	75	96	0.78	0.75	269	292
rs4804063	8082945	0.38 (0.38)	0.54 (0.54)	0.27	0.89	0.62	1.28	1 (1)	0.17	0.19	59	73	0.83	0.81	285	313
rs2086149	8083620	0.03 (0.05)	0.87 (0.83)	0.06	0.97	0.71	1.33	1 (1)	0.30	0.30	104	114	0.70	0.70	240	270
rs35579498	8089871	0.02 (0.02)	0.89 (0.89)	0.05	1.06	0.49	2.26	1 (1)	0.04	0.04	14	15	0.96	0.96	328	371
rs4527136	8092519	0.54 (0.54)	0.46 (0.46)	0.34	1.12	0.83	1.50	1 (1)	0.46	0.44	159	169	0.54	0.56	183	217
rs35840170	8094812	0.35 (0.35)	0.55 (0.55)	0.26	1.30	0.54	3.11	1 (1)	0.03	0.03	9	13	0.97	0.97	333	371
rs3813774	8102499	4.29 (4.36)	0.04 (0.04)	1.46	1.88	1.00	3.52	1 (1)	0.08	0.05	29	18	0.92	0.95	317	370
rs12974280	8102508	0.09 (0.09)	0.76 (0.76)	0.12	0.95	0.70	1.30	1 (1)	0.37	0.38	125	146	0.63	0.62	217	242
rs8112525	8107051	0.27 (0.29)	0.61 (0.59)	0.21	0.88	0.54	1.42	1 (1)	0.10	0.09	33	33	0.90	0.91	309	353
rs2061776	8108373	0.17 (0.17)	0.68 (0.68)	0.17	1.09	0.71	1.67	1 (1)	0.15	0.16	50	61	0.85	0.84	290	325
rs7246376	8109328	0.12 (0.12)	0.73 (0.73)	0.14	0.94	0.66	1.34	1 (1)	0.20	0.21	67	80	0.80	0.79	275	308
rs12162237	8113070	1.64 (1.64)	0.20 (0.20)	0.70	1.21	0.90	1.62	1 (1)	0.48	0.44	166	168	0.52	0.56	178	218
rs7252584	8113241	2.36 (2.36)	0.12 (0.12)	0.92	0.74	0.50	1.08	1 (1)	0.20	0.15	67	59	0.80	0.85	273	325
rs7256533	8113721	0.29 (0.29)	0.59 (0.59)	0.23	0.92	0.69	1.23	1 (1)	0.44	0.46	150	178	0.56	0.54	190	208

[a]Reference SNP cluster ID.
[b]Position of nucleotide on chromosome 19 in Build 35 of the human genome from UCSC (www.genome.ucsc.edu).
[c]Chi-squared values calculated using unphased 3.0.10 software.
[d]*P*-value of odds ratio.
[e]Odds ratios were calculated using unphased 3.0.10 software.
[f]Lower bound on the 95% confidence interval for the odds ratio.
[g]Upper bound on the 95% confidence interval for the odds ratio.
[h]*P*-value corrected for multiple testing (Bonferroni correction).
[i]Number of alleles in control subjects.
[j]Number of alleles in case subjects.

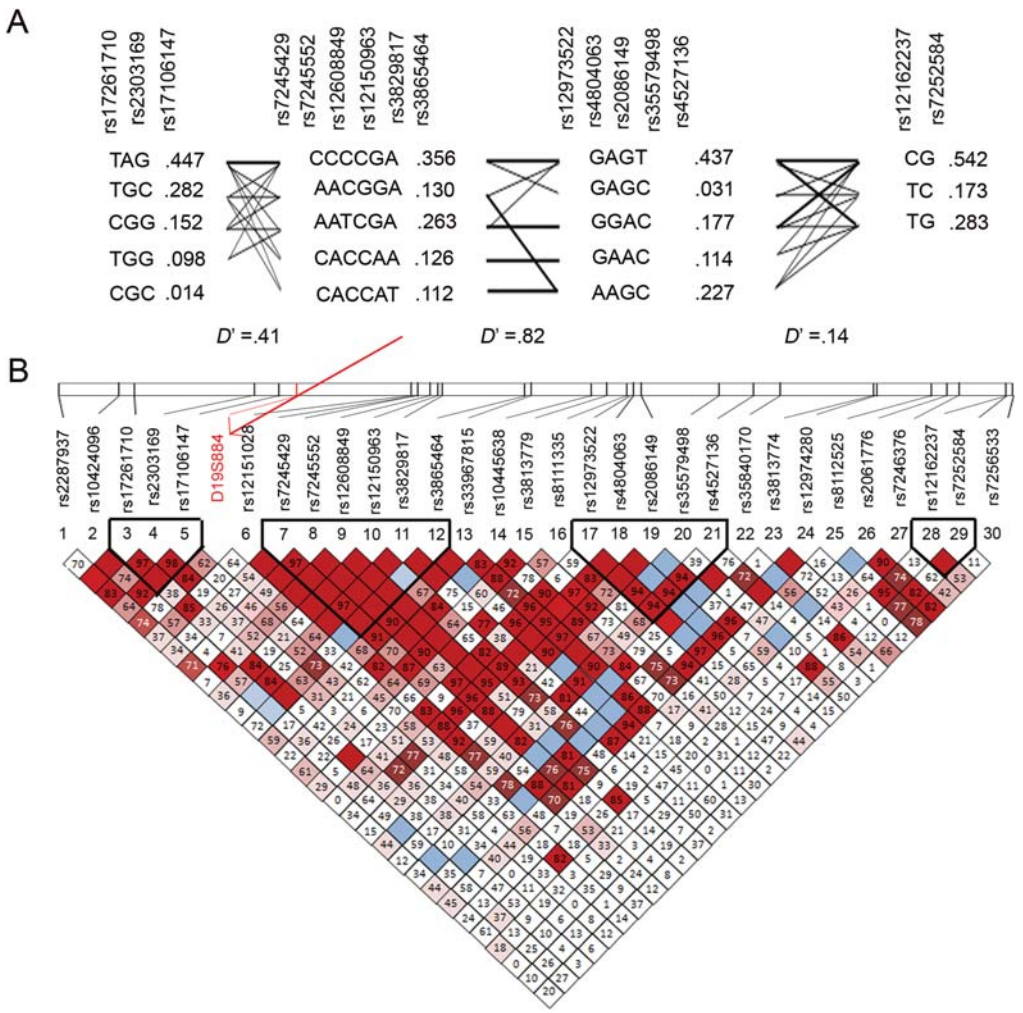

Figure 2 (**A**) Haplotypes predicted by Haploview. Four blocks were observed with the haplotpes of each block shown. Darker lines between haplotypes indicate a higher percentage of association with the linked haplotypes. Haplotype frequencies are indicated in red. D' values for LD are indicated below each haplotype block. Chromosomal positions were taken from those reported for build 35 of the UCSC genome website (http://www.genome.ucsc.edu/). (**B**) Haploview generated graphic analysis of LD in an 82 kb region of chromosome 19 spanning *FBN3*. The relative position of each of the 31 markers (30 SNPs and D19S884, which is indicated with an arrow) on chromosome 19p13.2 is indicated by the vertical lines on the **c**hromosomal map (top) and the proportion of LD (displayed as D'/LOD) is displayed below each marker. Haplotype blocks are indicated by dark lines. Strong LD ($D' = 1$, LOD ≥ 2) is indicated by red, lighter shades pink indicate varying degrees of LD with lighter shades displaying less than darker ($D' < 1$, LOD ≥ 2) and white indicates low LD ($D' < 1$, LOD < 2).

with PCOS. None of the 30 SNPs we tested had allele frequencies that were significantly different between controls and PCOS patients once corrected for multiple testing.

Microsatellite D19S884 is located in a non-conserved intronic region that displays low levels of LD, thus it remains possible that a causal SNP is located within this region. The closest SNP markers to D19S884 (chromosomal position 8056140) that were analysed here were rs17160147 and rs1251028, which are located at 2098 bp 3′ and 8784 bp 5′ of D19S884, respectively. There is at least one other SNP (rs1246064) in this region that was not analysed, nor captured by our tagging SNPs, and is heterogeneous in the CEU population. It is, however, unlikely that this SNP is causal for PCOS as it does not result in changes to protein sequence and was not found to be associated with PCOS in another study (Urbanek *et al.*, 2007). There are other SNPs in this region that are heterogeneous in either African (rs8102892, rs8112982), Asian (rs8105886, rs17160153) or both populations (rs17160151, rs12984611) but these are not heterogeneous in a European population and hence unlikely to be causal in an Australian population. As we did not find any SNP in the *FBN3* gene region that showed any significant association with PCOS, we examined the association of the microsatellite marker D19S884 in our cohort. Previous studies identified allele 8 (17 CA di-nucleotide repeats) as segregating with PCOS (Tucci *et al.*, 2001; Urbanek *et al.*, 2007). However, we were unable to identify any allele of the microsatellite that showed any significant association with PCOS in our cohort, after correcting for multiple testing.

The results presented here would appear to be in disagreement with other studies that found strong association between D19S884

Table IV For each allele in microsatellite D19S884 this table lists information on the sizes of the amplicons using either the current primers or those for amplimer AFMa299zc5, the numbers of CA repeats, the identification numbers ascribed to alleles by a previous study (Urbanek *et al.*, 2005), the frequencies of each allele listed in Genbank and in a previous study (Villuendas *et al.*, 2003) and that obtained in the current experiment, and the *P*-value for association of an allele with PCOS calculated using Fisher's exact test

Amplicon sizes*		Number of CA repeats	Allele identification number		Allele frequency									
Current data	Amplimer AFMa299zc5		Urbanek *et al.*	Genbank	Genbank†	Data of Villuendas *et al.*		Current data						
						Controls	PCOS	Controls (number of alleles)	PCOS (number of alleles)	*P*-value[a]	Odds ratio	95% low[b]	95% high[c]	Corrected *P*-value[d]
	214	12				–	0.01							
	216	13				0.01	–							
160	218	14	A5	10	0.12	0.07	0.01	0.09 (33)	0.06 (21)	0.26	1.44	1.22	1.69	1.00
162	220	15	A6	7	0.02	–	0.01	0.02 (6)	0.01 (5)	1.00	1.07	0.52	2.22	1.00
164	222	16	A7	2	0.11	0.12	0.07	0.10 (38)	0.12 (40)	0.47	0.83	0.74	0.93	1.00
166	224	17	A8	4	0.12	0.11	0.12	0.17 (64)	0.17 (60)	0.77	0.94	0.87	1.02	1.00
168	226	18	A9	1	0.12	0.17	0.13	0.12 (46)	0.13 (44)	0.74	0.92	0.84	1.02	1.00
170	228	19	A10	9	0.05	0.08	0.03	0.06 (22)	0.03 (9)	0.04	2.25	1.64	3.09	0.52
172	230	20	A11	3	0.11	0.09	0.11	0.11 (42)	0.11 (42)	1.00	0.98	0.88	1.10	1.00
174	232	21	A12	6	0.04	0.04	0.07	0.05 (18)	0.06 (20)	0.51	0.79	0.64	0.99	1.00
176	234	22	A13	5	0.25	0.27	0.28	0.26 (99)	0.27 (94)	0.62	0.92	0.87	0.97	1.00
178	236	23	A14	8	0.05	0.03	0.05	0.03 (13)	0.01 (4)	0.05	2.96	1.54	5.68	0.63
180	238	24				0.02	0.03	0.01 (4)	0.03 (9)	0.16	0.39	0.19	0.80	1.00
182	240	25						<0.00 (1)	0.00 (0)	1.00	–	–	–	1.00

*To detect microsatellite D19S884 we designed different primers (Table I) to that of amplimer AFMa299zc5 listed in Genbank, hence the current amplicons differ in size.
†Frequencies of alleles listed in Genbank are from 8 CEPH families composed of 56 individuals as described for the microsatellite polymorphism rs3222751 under reference submission ss4914553.
[a]*P*-value for association of a microsatellite allele with PCOS calculated by Fisher's exact test.
[b]Lower bound on the 95% confidence interval for the odds ratio.
[c]Upper bound on the 95% confidence interval for the odds ratio.
[d]*P*-value corrected for multiple testing (Bonferroni correction).

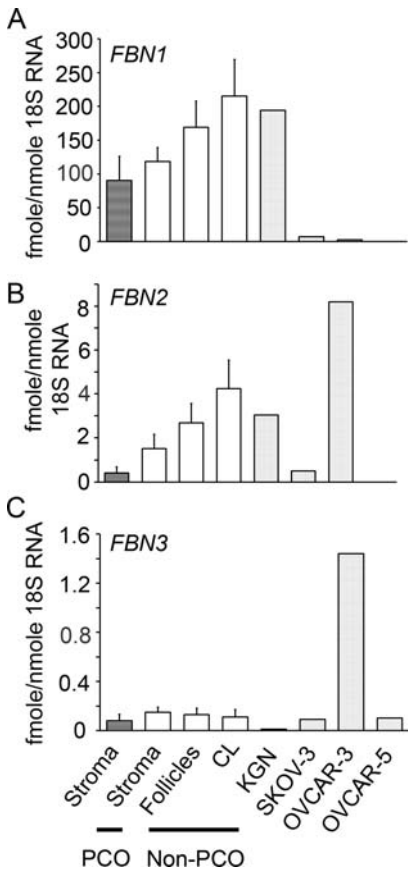

Figure 3 Expression of *FBN1* (**A**), *FBN2* (**B**) and *FBN3* (**C**) mRNA in human ovarian tissues and from the human ovarian tumour cell lines KGN, OVCAR-3, OVCAR-5 and SKOV-3. Data are presented as the mean values ± SEM expressed as fmoles RNA/nmole 18S ribosomal RNA, $n = 4$, 9, 3 and 3 for the PCO stroma/cortex and non-PCO stroma/cortex, follicles and corpora lutea (CL), respectively.

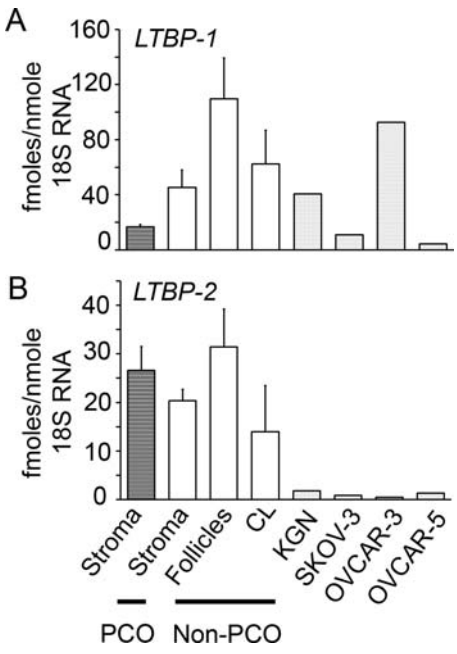

Figure 4 Expression of *LTBP-1* (**A**) and *LTBP-2* (**B**) mRNA in human ovarian tissues and from the human ovarian tumour cell lines KGN, OVCAR-3, OVCAR-5 and SKOV-3. Data are presented as the mean values ± SEM expressed as fmoles RNA/nmole 18S ribosomal RNA, $n = 4$, 9, 3 and 3 for the PCO stroma/cortex and non-PCO stroma/cortex, follicles and corpora lutea (CL), respectively.

and PCOS (Tucci *et al.*, 2001; Urbanek *et al.*, 2007). Both studies were conducted on subjects recruited solely from the USA and who fulfilled the 1990 NIH criteria. One study (Tucci *et al.*, 2001) was a case–control study whereas the other (Urbanek *et al.*, 2007) was a family-based study. We also recruited subjects of Caucasian background from the Australian population who fulfilled the 1990 NIH criteria for a case–control study. It is possible but unlikely that there are differences in genetic background with regard to PCOS between the Australian population and that of the USA. While the number of subjects in our study is low, our power calculations suggest that we had enough power to detect mutations that have a moderate (0.3) effect size and our numbers are much higher (173/194 PCOS/control subjects) than two previous case–control studies (Tucci *et al.*, 2001; Villuendas *et al.*, 2003) having 85/87 and 108/66 PCOS/control subjects, respectively. Our study is therefore more likely to be reflective of population allele frequencies and less prone to sampling bias. Despite this, it is possible that our numbers were too low to detect association of D19S884 with PCOS in the Australian population.

The expression of *FBN1, 2* and *3* and *LTBP-1* and *-2* were examined in PCO ovarian stroma/cortex and non-PCO stroma/cortex, follicles and corpora lutea and clear patterns emerged. Firstly, there were no differences between stroma from ovaries with a PCO phenotype and those from non-PCO ovaries in any of the genes examined. In all the tissues examined, the expression of *FBN1* was far greater than *FBN2*, which was far greater than *FBN3*, which was barely detectible. A similar pattern of expression was previously observed in bovine tunica and stroma of the cortex (Prodoehl *et al.*, 2009). In our previous study, we found that in the bovine ovary, the expression of *FBN1* within follicles was confined to the theca interna and in the tunica and stroma (corpora lutea were not examined) (Prodoehl *et al.*, 2009). In the current study we found that the expression of *LTBP-1* was greater than that of LTBP-2, which was also observed in the bovine tunica and stroma of the cortex (Prodoehl *et al.*, 2009). In bovine ovaries, the expression of *LTBP-1* was localized to the tunica and stroma of the cortex and in follicles in the inner area of the theca externa (Prodoehl *et al.*, 2009). Additionally, the immunolocalization pattern of *FBN1* and *LTBP-1* were fibrillar in the tunica and stroma of the cortex and in the thecal layers, suggesting that they are both associated with microfibrils as has been observed previously (Isogai *et al.*, 2003). Expression of *FBN1* and *2* and *LTBP-1* in the ovarian tissues examined here were correlated with each other. In bovine tunica and cortical stromal samples all three *FBN*s were correlated with *LTBP-2* and not *LTBP-1* (Prodoehl *et al.*, 2009). This suggests that there is some degree of coordinate regulation amongst these genes in both humans and in the bovine.

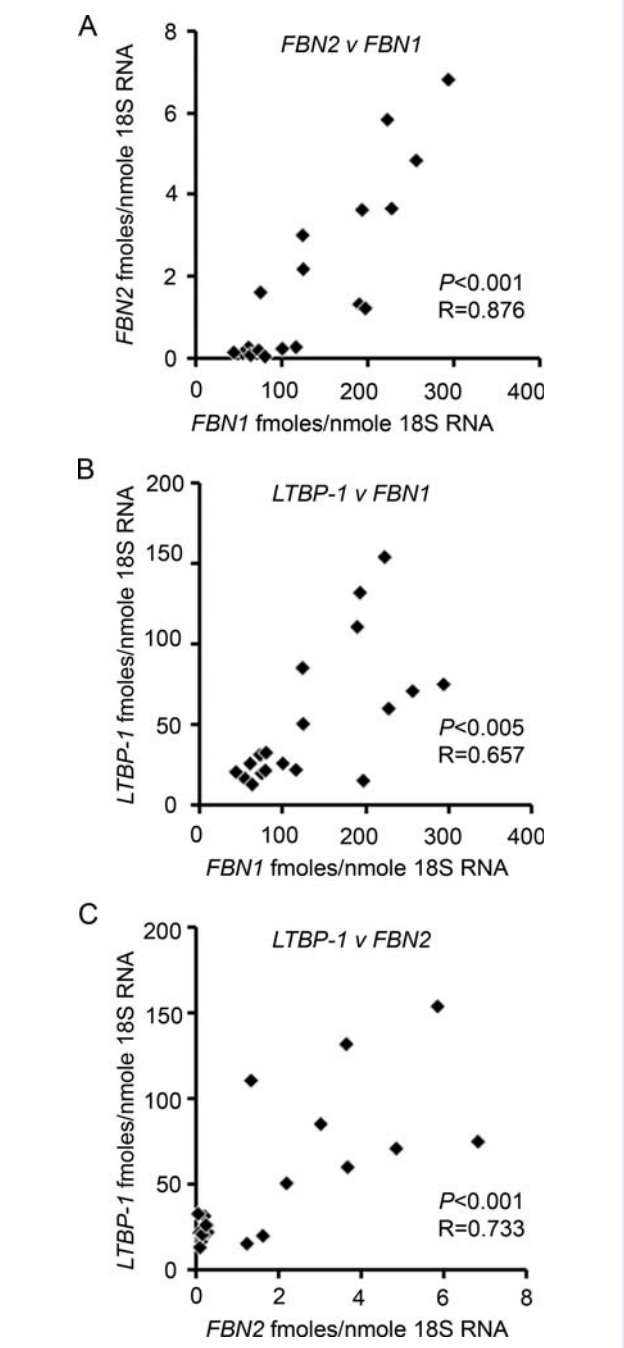

Figure 5 Scatter plots of (**A**) *FBN2* versus *FBN1*, (**B**) *LTBP-1* versus *FBN1* and (**C**) *LTBP-1* versus *FBN2* mRNA expression (fmoles/nmole 18S ribosomal RNA) using human ovarian tissues (excluding cell lines; $n = 19$). The *P*-values and correlation coefficient (*R*) relate to correlation with a Pearson's two-tailed test.

To increase our knowledge of fibrillin family members in ovaries expression was also examined in human ovarian cancer cell lines OVCAR-3, OVCAR-5 and SKOV-3 (ascites derived) derived from ovarian adenocarcinoma, and in KGN cells which have a granulosa cell phenotype (Nishi *et al*., 2001). The expression levels of *FBN1*, *2* and *3* and *LTBP-1* in the KGN cells was generally similar to that of the other ovarian tissues examined. The expression of these genes was much lower in the OVCAR-5 and SKOV-3 cells, in agreement with the localization of *FBN1* and *LTBP-1* and *-2* in the bovine where no localization to the ovarian surface epithelium was observed (Prodoehl *et al*., 2009). However, OVCAR-3 had elevated levels of *FBN2*, *3*, and *LTBP-1* relative to normal ovarian tissues and other ovarian cancer cell lines.

It appears, from our genetic analysis, that the marker D19S884 and its associated gene, *FBN3*, have little or no impact on PCOS pathology in the Australian population. We cannot, however, rule out the possibility that other markers in the region of chromosome 19p13.2 are associated. Additionally our study of expression of five members of the fibrillin family in human ovaries found very low levels of *FBN3*, but our study also cannot rule out that alterations in *FBN3* expression occur in other organs or tissues such as the anterior pituitary, influencing hormonal regulation of the ovary or adipose tissue. It is also possible that a genetic lesion in the *FBN3* gene associated with PCOS pathology may cause functional changes in the protein's structure without affecting its expression levels. We conclude that if *FBN3* is involved in the aetiology of PCOS then its role is not readily apparent from these studies.

Authors' Role

M.J.P., N.H., H.F.I.-R., M.A.G. and R.J.R. planned the experiments, conducted RT–PCR, microsatellite analyses, statistical analysis and wrote the manuscript. Z.Z.Z., J.N.P. and G.W.M. conducted the SNP analysis and statistical analysis and assisted in writing the manuscript. T.E.H. and R.J.N. developed the cohort of PCOS and control patients, isolated the DNA from the lymphocytes from these patients, and reviewed the manuscript. W.E.R., B.R.C. and H.D.M. provided human ovarian samples and RNA and reviewed the manuscript.

Acknowledgements

We thank Professors Hajime Nawata and Toshihiko Yanase of Kyushu University and Professor Yoshihiro Nishi of Kurume University for the KGN cell line, Drs Suman Rice and Laura Pellatt for ovarian tissues, and Dr Carmela Ricciardelli and Miranda Ween for the cancer cell lines. Funding to pay the Open Access publication charges for this article was provided by the National Health and Medical Research Council of Australia.

Funding

Funding to support this research was obtained from the National Health and Medical Research Council of Australia, University of Adelaide, the Clive and Vera Ramaciotti Foundation, the Wellcome Trust, and National Institute of Health, and Medical Research Council UK.

References

Adams J, Polson DW, Franks S. Prevalence of polycystic ovaries in women with anovulation and idiopathic hirsutism. *Br Med J (Clin Res Ed)* 1986; **293**:355–359.

Amato P, Simpson JL. The genetics of polycystic ovary syndrome. *Best Pract Res Clin Obstet Gynaecol* 2004;**18**:707–718.

Balen AH, Conway GS, Kaltsas G, Techatrasak K, Manning PJ, West C, Jacobs HS. Polycystic ovary syndrome: the spectrum of the disorder in 1741 patients. *Hum Reprod* 1995;**10**:2107–2111.

Barrett JC, Fry B, Maller J, Daly MJ. Haploview: analysis visualization of LD haplotype maps. *Bioinformatics* 2005;**21**:263–265.

Boileau C, Jondeau G, Mizuguchi T, Matsumoto N. Molecular genetics of Marfan syndrome. *Curr Opin Cardiol* 2005;**20**:194–200.

Buchner A, Faul F, Erdfeldera E. *G Power: A Priori, Post-hoc, and Compromise Power Analyses for the Macintosh. University of Trier* 1997; (http://www.psychouni-duesseldorfde/app/projects/gpower).

Carey AH, Waterworth D, Patel K, White D, Little J, Novelli P, Franks S, Williamson R. Polycystic ovaries and premature male pattern baldness are associated with one allele of the steroid metabolism gene CYP17. *Hum Mol Genet* 1994;**3**:1873–1876.

Christner PJ, Ayitey S. Extracellular matrix containing mutated fibrillin-1 (Fbn1) down regulates Col1a1, Col1a2, Col3a1, Col5a1, and Col5a2 mRNA levels in Tsk/+ and Tsk/Tsk embryonic fibroblasts. *Amino Acids* 2006;**30**:445–451.

Conway GS, Honour JW, Jacobs HS. Heterogeneity of the polycystic ovary syndrome: clinical, endocrine and ultrasound features in 556 patients. *Clin Endocrinol (Oxf)* 1989;**30**:459–470.

Corson GM, Charbonneau NL, Keene DR, Sakai LY. Differential expression of fibrillin-3 adds to microfibril variety in human and avian, but not rodent, connective tissues. *Genomics* 2004;**83**:461–472.

Diamanti-Kandarakis E, Kouli CR, Bergiele AT, Filandra FA, Tsianateli TC, Spina GG, Zapanti ED, Bartzis MI. A survey of the polycystic ovary syndrome in the Greek island of Lesbos: hormonal and metabolic profile. *J Clin Endocrinol Metab* 1999;**84**:4006–4011.

Dudbridge F. Likelihood-for nuclear families and unrelated subjects with missing genotype data. *Hum Hered* 2008;**66**:87–98.

Franks S. Polycystic ovary syndrome. *N Engl J Med* 1995;**333**:853–861.

Gabriel SB, Schaffner SF, Nguyen H, Moore JM, Roy J, Blumenstiel B, Higgins J, DeFelice M, Lochner A, Faggart M *et al*. The structure of haplotype blocks in the human genome. *Science (New York, NY)* 2002;**296**:2225–2229.

Gharani N, Waterworth DM, Batty S, White D, Gilling-Smith C, Conway GS, McCarthy M, Franks S, Williamson R. Association of the steroid synthesis gene CYP11a with polycystic ovary syndrome and hyperandrogenism. *Hum Mol Genet* 1997;**6**:397–402.

Gibson MA, Hatzinikolas G, Davis EC, Baker E, Sutherland GR, Mecham RP. Bovine latent transforming growth factor beta 1-binding protein 2: molecular cloning, identification of tissue isoforms, and immunolocalization to elastin-associated microfibrils. *Mol Cell Biol* 1995;**15**:6932–6942.

Giltay R, Kostka G, Timpl R. Sequence and expression of a novel member (LTBP-4) of the family of latent transforming growth factor-beta binding proteins. *FEBS Lett* 1997;**411**:164–168.

Glister C, Richards SL, Knight PG. Bone morphogenetic proteins (BMP) -4, -6, and -7 potently suppress basal and luteinizing hormone-induced androgen production by bovine theca interna cells in primary culture: could ovarian hyperandrogenic dysfunction be caused by a defect in thecal BMP signaling? *Endocrinology* 2005;**146**:1883–1892.

Glister C, Groome NP, Knight PG. Bovine follicle development is associated with divergent changes in activin-A, inhibin-A and follistatin and the relative abundance of different follistatin isoforms in follicular fluid. *J Endocrinol* 2006;**188**:215–225.

Govinden R, Bhoola KD. Genealogy expression cellular function of transforming growth factor-beta. *Pharmacol Ther* 2003;**98**:257–265.

Hirani R, Hanssen E, Gibson MA. LTBP-2 specifically interacts with the amino-terminal region of fibrillin-1 competes with LTBP-1 for binding to this microfibrillar protein. *Matrix Biol* 2007;**26**:213–223.

Hughesdon PE. Morphology and morphogenesis of the Stein-Leventhal ovary and of so-called "hyperthecosis". *Obstet Gynecol Surv* 1982;**37**:59–77.

Isogai Z, Ono RN, Ushiro S, Keene DR, Chen Y, Mazzieri R, Charbonneau NL, Reinhardt DP, Rifkin DB, Sakai LY. Latent transforming growth factor beta-binding protein 1 interacts with fibrillin and is a microfibril-associated protein. *J Biol Chem* 2003;**278**:2750–2757.

Jones MR, Wilson SG, Mullin BH, Mead R, Watts GF, Stuckey BG. Polymorphism of the follistatin gene in polycystic ovary syndrome. *Mol Hum Reprod* 2007;**13**:237–241.

Kanzaki T, Olofsson A, Moren A, Wernstedt C, Hellman U, Miyazono K, Claesson-Welsh L, Heldin CH. TGF-beta 1 binding protein: a component of the large latent complex of TGF-beta 1 with multiple repeat sequences. *Cell* 1990;**61**:1051–1061.

Kevenaar ME, Laven JS, Fong SL, Uitterlinden AG, de Jong FH, Themmen AP, Visser JA. A functional anti-mullerian hormone gene polymorphism is associated with follicle number and androgen levels in polycystic ovary syndrome patients. *J Clin Endocrinol Metab* 2008;**93**:1310–1316.

Kielty CM, Sherratt MJ, Shuttleworth CA. Elastic fibres. *J Cell Sci* 2002;**115**:2817–2828.

Knochenhauer ES, Key TJ, Kahsar-Miller M, Waggoner W, Boots LR, Azziz R. Prevalence of the polycystic ovary syndrome in unselected black and white women of the southeastern United States: a prospective study. *J Clin Endocrinol Metab* 1998;**83**:3078–3082.

Lee B, Godfrey M, Vitale E, Hori H, Mattei MG, Sarfarazi M, Tsipouras P, Ramirez F, Hollister DW. Linkage of Marfan syndrome and a phenotypically related disorder to two different fibrillin genes. *Nature* 1991;**352**:330–334.

Legro RS, Bentley-Lewis R, Driscoll D, Wang SC, Dunaif A. Insulin resistance in the sisters of women with polycystic ovary syndrome: association with hyperandrogenemia rather than menstrual irregularity. *J Clin Endocrinol Metab* 2002;**87**:2128–2133.

Mason HD, Willis DS, Beard RW, Winston RM, Margara R, Franks S. Estradiol production by granulosa cells of normal and polycystic ovaries: relationship to menstrual cycle history and concentrations of gonadotropins and sex steroids in follicular fluid. *J Clin Endocrinol Metab* 1994;**79**:1355–1360.

Milner CR, Craig JE, Hussey ND, Norman RJ. No association between the -308 polymorphism in the tumour necrosis factor alpha (TNFalpha) promoter region and polycystic ovaries. *Mol Hum Reprod* 1999;**5**:5–9.

Miyazono K, Olofsson A, Colosetti P, Heldin CH. A role of the latent TGF-beta 1-binding protein in the assembly and secretion of TGF-beta 1. *Embo J* 1991;**10**:1091–1101.

Moren A, Olofsson A, Stenman G, Sahlin P, Kanzaki T, Claesson-Welsh L, ten Dijke P, Miyazono K, Heldin CH. Identification and characterization of LTBP-2, a novel latent transforming growth factor-beta-binding protein. *J Biol Chem* 1994;**269**:32469–32478.

Neptune ER, Frischmeyer PA, Arking DE, Myers L, Bunton TE, Gayraud B, Ramirez F, Sakai LY, Dietz HC. Dysregulation of TGF-beta activation contributes to pathogenesis in Marfan syndrome. *Nat Genet* 2003;**33**:407–411.

Nishi Y, Yanase T, Mu Y, Oba K, Ichino I, Saito M, Nomura M, Mukasa C, Okabe T, Goto K *et al*. Establishment and characterization of a steroidogenic human granulosa-like tumor cell line, KGN, that expresses functional follicle-stimulating hormone receptor. *Endocrinology* 2001;**142**:437–445.

Prodoehl MJ, Irving-Rodgers HF, Bonner W, Sullivan TM, Micke GC, Gibson MA, Perry VE, Rodgers RJ. Fibrillins and latent TGFβ binding proteins in bovine ovaries of offspring following high or low protein diets during pregnancy of dams. *Mol Cell Endocrinol* 2009;**307**:133–144.

Ramirez F, Pereira L. The fibrillins. *Int J Biochem Cell Biol* 1999;**31**:255–259.
Sakai LY, Keene DR, Engvall E. Fibrillin, a new 350-kD glycoprotein, is a component of extracellular microfibrils. *J Cell Biol* 1986;**103**:2499–2509.
Slowinska-Srzednicka J, Zgliczynski S, Wierzbicki M, Srzednicki M, Stopinska-Gluszak U, Zgliczynski W, Soszynski P, Chotkowska E, Bednarska M, Sadowski Z. The role of hyperinsulinemia in the development of lipid disturbances in nonobese and obese women with the polycystic ovary syndrome. *J Endocrinol Invest* 1991;**14**:569–575.
Talbott E, Guzick D, Clerici A, Berga S, Detre K, Weimer K, Kuller L. Coronary heart disease risk factors in women with polycystic ovary syndrome. *Arterioscler Thromb Vasc Biol* 1995;**15**:821–826.
Thompson TB, Lerch TF, Cook RW, Woodruff TK, Jardetzky TS. The structure of the follistatin:activin complex reveals antagonism of both type I and type II receptor binding. *Dev Cell* 2005;**9**:535–543.
Tucci S, Futterweit W, Concepcion ES, Greenberg DA, Villanueva R, Davies TF, Tomer Y. Evidence for association of polycystic ovary syndrome in caucasian women with a marker at the insulin receptor gene locus. *J Clin Endocrinol Metab* 2001;**86**:446–449.
Urbanek M, Legro RS, Driscoll DA, Azziz R, Ehrmann DA, Norman RJ, Strauss JF 3rd, Spielman RS, Dunaif A. Thirty-seven candidate genes for polycystic ovary syndrome: strongest evidence for linkage is with follistatin. *Proc Natl Acad Sci U S A* 1999;**96**:8573–8578.
Urbanek M, Wu X, Vickery KR, Kao LC, Christenson LK, Schneyer A, Legro RS, Driscoll DA, Strauss JF 3rd, Dunaif A *et al.* Allelic variants of the follistatin gene in polycystic ovary syndrome. *J Clin Endocrinol Metab* 2000;**85**:4455–4461.
Urbanek M, Woodroffe A, Ewens KG, Diamanti-Kandarakis E, Legro RS, Strauss JF 3rd, Dunaif A, Spielman RS. Candidate gene region for polycystic ovary syndrome on chromosome 19p13.2. *J Clin Endocrinol Metab* 2005;**90**:6623–6629.
Urbanek M, Sam S, Legro RS, Dunaif A. Identification of a polycystic ovary syndrome susceptibility variant in fibrillin-3 and association with a metabolic phenotype. *J Clin Endocrinol Metab* 2007;**92**:4191–4198.
Verrecchia F, Mauviel A. TGF-beta and TNF-alpha: antagonistic cytokines controlling type I collagen gene expression. *Cell Signal* 2004;**16**:873–880.
Villuendas G, Escobar-Morreale HF, Tosi F, Sancho J, Moghetti P, San Millan JL. Association between the D19S884 marker at the insulin receptor gene locus and polycystic ovary syndrome. *Fertil Steril* 2003; **79**:219–220.
Wang S, Chen Q, Simon TC, Strebeck F, Chaudhary L, Morrissey J, Liapis H, Klahr S, Hruska KA. Bone morphogenic protein-7 (BMP-7), a novel therapy for diabetic nephropathy. *Kidney Int* 2003;**63**:2037–2049.
Wheeler DL, Church DM, Federhen S, Lash AE, Madden TL, Pontius JU, Schuler GD, Schriml LM, Sequeira E, Tatusova TA *et al.* Database resources of the National Center for Biotechnology. *Nucleic Acids Res* 2003;**31**:28–33.
Wild RA, Bartholomew MJ. The influence of body weight on lipoprotein lipids in patients with polycystic ovary syndrome. *Am J Obstet Gynecol* 1988;**159**:423–427.
Wild RA, Painter PC, Coulson PB, Carruth KB, Ranney GB. Lipoprotein lipid concentrations and cardiovascular risk in women with polycystic ovary syndrome. *J Clin Endocrinol Metab* 1985;**61**:946–951.
Wild RA, Alaupovic P, Parker IJ. Lipid and apolipoprotein abnormalities in hirsute women. I. The association with insulin resistance. *Am J Obstet Gynecol* 1992;**166**:1191–1196. Discussion 1196–1197.
Yildiz BO, Yarali H, Oguz H, Bayraktar M. Glucose intolerance, insulin resistance, and hyperandrogenemia in first degree relatives of women with polycystic ovary syndrome. *J Clin Endocrinol Metab* 2003;**88**: 2031–2036.
Yin W, Smiley E, Germiller J, Mecham RP, Florer JB, Wenstrup RJ, Bonadio J. Isolation of a novel latent transforming growth factor-beta binding protein gene (LTBP-3). *J Biol Chem* 1995;**270**:10147–10160.
Zawadski JK, Dunaif A. Diagnostic criteria for polycystic ovary syndrome: towards a rational approach. In: Dunaif A, Givens JR, Haseltine FR (eds). Boston: Blackwell Scientific, 1992, 377–384.
Zeisberg M, Bottiglio C, Kumar N, Maeshima Y, Strutz F, Muller GA, Kalluri R. Bone morphogenic protein-7 inhibits progression of chronic renal fibrosis associated with two genetic mouse models. *Am J Physiol* 2003;**285**:F1060–F1067.
Zhao ZZ, Nyholt DR, Le L, Martin NG, James MR, Treloar SA, Montgomery GW. KRAS variation and risk of endometriosis. *Mol Hum Reprod* 2006;**12**:671–676.

Submitted on May 13, 2009; resubmitted on August 11, 2009; accepted on August 17, 2009